J Mol Model (2011) 17:777–784
DOI 10.1007/s00894-010-0761-1

ORIGINAL PAPER

Potential use of some metal clusters as hydrogen storage materials—a conceptual DFT approach

Santanab Giri · Arindam Chakraborty · Pratim Kumar Chattaraj

Received: 7 March 2010 / Accepted: 17 May 2010 / Published online: 16 June 2010

Abstract Structure, stability and reactivity of several metal clusters with or without hydrogen doping were studied using standard ab initio and density functional theory (DFT) calculations. Conceptual DFT-based reactivity descriptors and the associated electronic structure principles lend additional support towards understanding the stability of metal clusters upon hydrogen doping. Related aromaticity was analyzed through nucleus-independent chemical shift values. Site selectivity towards electrophilic and nucleophilic attacks were analyzed in terms of the corresponding local reactivity descriptors. Most of the metal clusters have the capacity to trap hydrogen molecules.

Keywords Hydrogen storage · Metal cluster · Conceptual DFT · Aromaticity

Introduction

A global boom in population in the last couple of decades has led to several social as well as environmental problems for the human race. Vigorous deforestation and unparalleled industrialization worldwide have improved the economic "sensex"[1] on the one hand, but on the other, mankind has been gifted with global warming—a never-ending environmental hazard. Excessive use of fossil fuels has already made a deep impact on natural energy reserves. Thus, the probable upcoming energy crisis and its possible remedies have become a topic of great concern for every conscious scientific mind. The use of solar cells and other materials as non-conventional energy resources have already been employed. There are also further thrusts to develop alternative clean energy resources [1–3]. Hydrogen, the third most abundant element on Earth, has been found to be a clean and convenient environmentally friendly energy carrier for future use in the automobile industry and is a good substitute for fossil fuel resources. However, the lack of appropriate materials for the physical storage of hydrogen in large gravimetric and volumetric densities is the primary reason limiting its extensive use in practice. Nonetheless, several materials, such as aluminum nitride (AlN) nanostructures [4], transition-metal doped boron nitride (BN) systems [5], alkali-metal doped benzenoid [6] and fullerene clusters [7], bare as well as light metal and transition-metal coated boron buckyballs, B_{80} [8], and magnesium clusters [9] have been tested experimentally and theoretically as potential storage materials for hydrogen. Again, owing to the considerable capacity of MgH_2 as a hydrogen-storage material, Mg-clusters doped with H_2 molecules have been investigated theoretically and found to be weakly stable or metastable depending on the cluster size [10].

In this article, we have made an attempt to invoke the use of the cage-like Mg-clusters predicted by McNelles et al. [10] and similar Ca-analogues (see below) of those Mg cages as potential traps for hydrogen. The trigonal alkali-metal

Electronic supplementary material The online version of this article (doi:10.1007/s00894-010-0761-1) contains supplementary material, which is available to authorized users.

S. Giri · A. Chakraborty · P. K. Chattaraj (✉)
Department of Chemistry and Center for Theoretical Studies,
Indian Institute of Technology,
Kharagpur,
Kharagpur 721302, India
e-mail: pkc@chem.iitkgp.ernet.in

[1] Sensex is an abbreviation for the Bombay Exchange Sensitive Index—the benchmark index of the Bombay Stock Exchange (BSE).

cationic clusters, Li_3^+ and Na_3^+ were also investigated for their ability to bind hydrogen in its molecular form. The practical ability of these small trigonal or medium cage-clusters as storage materials for hydrogen can be judged from changes in aspects of their structure and

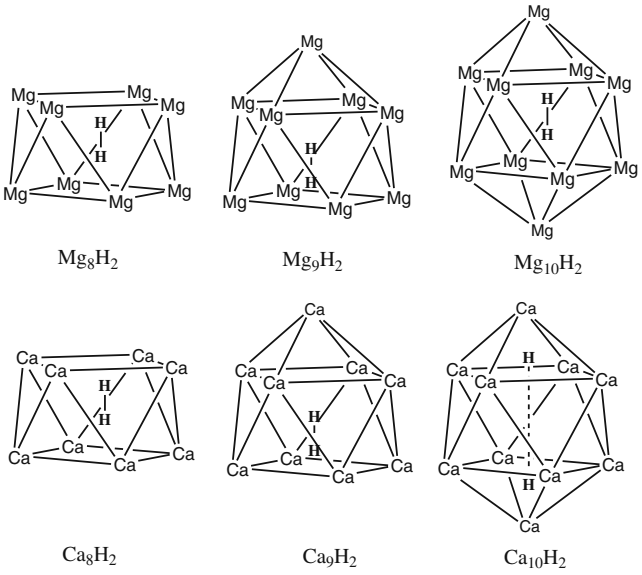

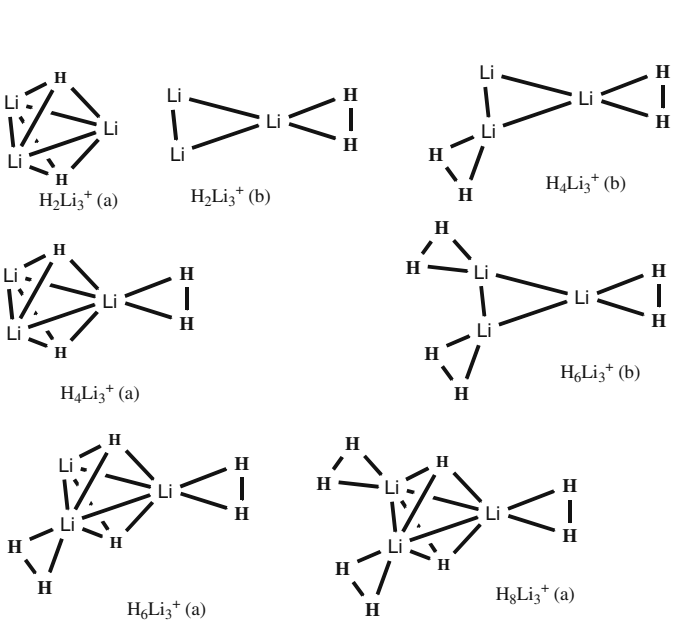

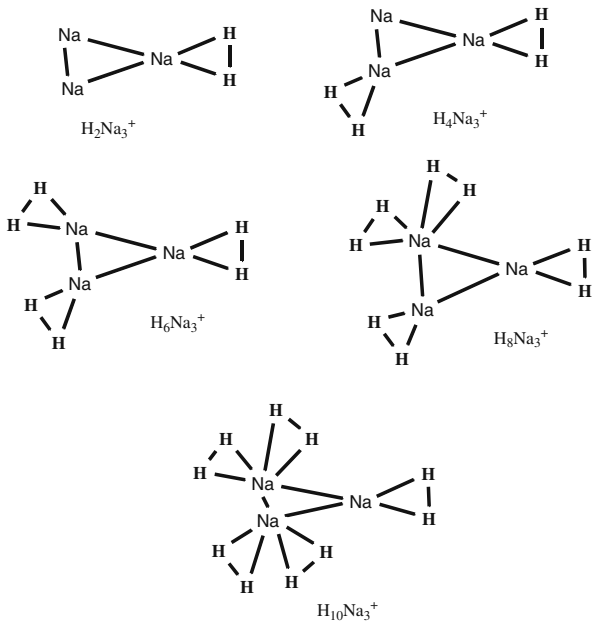

stability comparing the free, un-bound to the H_2-trapped form. Conceptual density functional theory (DFT) [11–14] in conjunction with its various global reactivity descriptors, like electronegativity [15–17] (χ), hardness [18–20] (η), electrophilicity [21–23] (ω), and its local variants, like atomic charges [24] (Q_k) and Fukui functions [25] (f_k), can elucidate the stability and associated structural changes of the metal clusters upon binding with molecular hydrogen. Further, an assessment of the aromaticity criterion in the trigonal rings of Li_3^+ and Na_3^+ as well as for the Mg/Ca rings in the cage-clusters measured in terms of the nucleus independent chemical shift (NICS) [26] values provide ample evidence to justify the stability of the H_2-bound metal clusters theoretically.

Theoretical background

The thermodynamic stability of any chemical system, irrespective of its size, may be assessed quantitatively from its chemical hardness (η) and electrophilicity (ω) values. This

Table 1 Energy (E, a.u.), electronegativity (χ, eV), hardness (η, eV) and electrophilicity (ω, eV) of different H_2-trapped Mg_n and Ca_n cages

Molecule	E, au	χ, eV	η, eV	ω, eV
H_2Mg_8	−1,601.94845	3.280	2.233	2.409
H_2Mg_9	−1,802.07050	3.358	2.270	2.483
H_2Mg_{10}	−2,002.16655	3.085	2.082	2.286
H_2Ca_8	−5,421.87014	2.639	1.629	2.138
H_2Ca_9	−6,099.48777	2.638	1.609	2.163
H_2Ca_{10}	−6,777.15355	2.728	1.514	2.459

has well been justified by the establishment of various electronic structure principles like the principles of maximum hardness [27–29] (PMH), minimum polarizability [30, 31] (PMP) and minimum electrophilicity [32, 33] (PME). The above structure principles play a major role in determining the changes in stability of the metal clusters from their free, unbound state to the corresponding H_2-trapped form. In an N-electron system, electronegativity [15–17] (χ) and hardness [18–20] (η) can be defined as follows:

$$\chi = -\mu = -\left(\frac{\partial E}{\partial N}\right)_{v(\vec{r})} \tag{1}$$

$$\eta = \left(\frac{\partial^2 E}{\partial N^2}\right)_{v\left(\vec{r}\right)} \tag{2}$$

Here, E is the total energy of the N-electron system and μ, and $v\left(\vec{r}\right)$ are its chemical potential and external potential, respectively. Electrophilicity [21–23] (ω) is defined as:

$$\omega = \frac{\mu^2}{2\eta} = \frac{\chi^2}{2\eta} \tag{3}$$

A finite difference approximation to Eqs. 1 and 2 can be expressed as:

Table 2 Electronegativity (χ, eV), hardness (η, eV) and electrophilicity (ω, eV) of H_2, Li_3^+ and the different H_2-trapped Li_3^+ clusters (types a and b, as indicated)

Molecule	χ (eV)	η (eV)	ω (eV)
H_2	6.400	20.530	0.998
Li_3^+	7.345	6.444	4.185
H_2-Li_3^+ (a)	8.871	9.667	4.071
H_2-Li_3^+ (b)	7.232	6.363	4.110
H_4-Li_3^+ (a)	8.783	9.572	4.029
H_4-Li_3^+ (b)	7.065	6.398	3.901
H_6-Li_3^+ (a)	8.659	9.550	3.926
H_6-Li_3^+ (b)	6.847	6.527	3.591
H_8-Li_3^+ (a)	8.414	9.775	3.621

Table 3 Electronegativity (χ, eV), hardness (η, eV) and electrophilicity (ω, eV) of H_2, Na_3^+ and the different H_2-trapped Na_3^+ clusters

Molecule	χ (eV)	η (eV)	ω (eV)
Na_3^+	6.870	5.887	4.009
H_2-Na_3^+	6.798	5.870	3.936
H_4-Na_3^+	6.695	5.920	3.786
H_6-Na_3^+	6.555	6.047	3.553
H_8-Na_3^+	6.513	6.007	3.531
H_{10}-Na_3^+	6.457	6.013	3.466

$$\chi = \frac{I + A}{2} \tag{4}$$

and

$$\eta = I - A \tag{5}$$

where I and A represent the ionization potential and electron affinity of the system, respectively, and are computed in terms of the energies of the N and $N\pm1$ electron systems. For an N-electron system with energy E (N) they may be expressed as follow:

$$I = E(N-1) - E(N) \tag{6}$$

and

$$A = E(N) - E(N+1) \tag{7}$$

The local reactivity descriptor, Fukui function [25] (FF), measures the change in electron density at a given point when an electron is added to or removed from a system at constant $v\left(\vec{r}\right)$. It may be written as:

$$f\left(\vec{r}\right) = \left(\frac{\partial \rho\left(\vec{r}\right)}{\partial N}\right)_{v\left(\vec{r}\right)} = \left(\frac{\delta \mu}{\delta v\left(\vec{r}\right)}\right)_N \tag{8}$$

Condensation of this Fukui function, $f\left(\vec{r}\right)$ to an individual atomic site k in a molecule gives rise to the following expressions in terms of electron population [34] q_k:

$$f_k^+ = q_k(N+1) - q_k(N) \text{ for nucleophilic attack} \tag{9a}$$

$$f_k^- = q_k(N) - q_k(N-1) \text{ for electrophilic attack} \tag{9b}$$

$$f_k^o = [q_k(N+1) - q_k(N-1)]/2 \text{ for radical attack} \tag{9c}$$

Table 4 Energies of H_2, Li_3^+ and the different H_2-trapped Li_3^+ clusters (types a and b) at different levels of theory

Complex	B3LYP 6–311+G(d)	MP2 6–311+G(d)	B3LYP cc-pvdz
H_2	−1.17663	−1.14588	−1.17360
Li_3^+	−22.37210	−22.19253	−22.37184
H_2-Li_3^+ (a)	−23.60003	−23.38082	−23.60359
H_4-Li_3^+ (a)	−24.78252	−24.53302	−24.77395
H_6-Li_3^+ (a)	−25.96494	−25.68516	−22.95520
H_8-Li_3^+ (a)	−27.14728	−26.83725	−27.16389
H_2-Li_3^+ (b)	−23.55273	−23.34260	−23.55927
H_4-Li_3^+ (b)	−24.73310	−24.49243	−24.74399
H_6-Li_3^+ (b)	−25.91319	−25.64199	−25.92838

Table 5 Energies of Na_3^+ and the different H_2-trapped Na_3^+ clusters at different levels of theory

	B3LYP	MP2	B3LYP
Complexes	6−311+G(d)	6−311+G(d)	cc−pvdz
Na_3^+	−486.74661	−485.42563	−486.75902
H_2-Na_3^+	−487.92436	−486.57260	−487.93505
H_4-Na_3^+	−489.10201	−487.71947	−489.11097
H_6-Na_3^+	−490.27954	−488.86626	−490.28675
H_8-Na_3^+	−491.45650	−490.01260	−491.46185
H_{10}-Na_3^+	−492.63339	−491.15889	−492.63685

Table 6 Nucleus independent chemical shift (NICS [0, 1 (ppm)] for the upper and lower rings of different H_2-trapped Mg_n and Ca_n cages

Molecule	NICS(0) Upper	NICS(0) Lower	NICS(1) Upper	NICS(1) Lower
H_2Mg_8	−12.72	−12.72	−9.12	−9.09
H_2Mg_9	−47.90	−52.70	−17.99	−47.82
H_2Mg_{10}	−35.40	−35.32	−14.79	−14.86
H_2Ca_8	−4.92	−4.57	−4.58	−4.31
H_2Ca_9	−39.00	−36.83	−35.05	−10.92
H_2Ca_{10}	−62.33	−62.27	−36.93	−36.66

Table 7 $NICS_{ZZ}$ (0, ppm) values of the trigonal Li_3 ring in the different H_2-trapped Li_3^+ (types a and b) clusters

Molecule	NICSzz(0)
Li_3^+	−8.75
H_2-Li_3^+ (a)	−14.57
H_4-Li_3^+ (a)	−14.44
H_6-Li_3^+ (a)	−14.32
H_8-Li_3^+ (a)	−14.19
H_2-Li_3^+ (b)	−8.49
H_4-Li_3^+ (b)	−11.97
H_6-Li_3^+ (b)	−7.87

Table 9 Reaction energy (ΔE, kcal mol^{-1}) for the gradual formation of different H_2-trapped Li_3^+ (types a and b) clusters

Reaction	ΔE
$Li_3^+ + H_2 = H_2Li_3^+$ (a)	−32.188
$H_2Li_3^+$ (a) + $H_2 = H_4Li_3^+$ (a)	−3.677
$H_4Li_3^+$ (a) + $H_2 = H_6Li_3^+$ (a)	−3.631
$H_6Li_3^+$ (a) + $H_2 = H_8Li_3^+$ (a)	−3.584
$Li_3^+ + H_2 = H_2Li_3^+$ (b)	−2.508
H_2-Li_3^+ (b) + $H_2 = H_4Li_3^+$ (b)	−2.346
H_4-Li_3^+ (b) + $H_2 = H_6Li_3^+$ (b)	−2.168

Computational details

Geometry optimization of the different H_2-trapped Mg_n and Ca_n cages (n=8–10) was performed at the B3LYP/6–311+G(d) level of theory. For the various conformers of Li_3^+ and Na_3^+-bound poly-hydrogen clusters, optimization of the molecular geometry was carried out at the B3LYP/cc-pvdz, B3LYP/6–311+G(d) and MP2/6–311+G(d) levels of theory. All computations were performed using the GAUSSIAN 03 program package [35]. The number of imaginary frequencies (NIMAG) of all the optimized geometries is zero, thereby confirming their existence at the minima on the potential energy surface (PES). Single point calculations were further done to evaluate the energies of the $N\pm1$ electron systems by adopting the geometries of the corresponding N-electron systems optimized at the B3LYP/6–311+G(d) level of theory. The I and A values were calculated using a ΔSCF technique. The electrophilicity (ω) and hardness (η) were computed using Eqs. 3 and 5, respectively. A Mulliken population analysis (MPA) scheme was adopted to calculate the atomic charges (Q_k) and FFs $\left(f\left(r\right)\right)$. The NICS [26] values [NICS(0, 1)] of the upper and lower rings of the H_2-bound Mg_n and Ca_n cages (n=8–10) as well as the [$NICS_{zz}$(0)] for the free and H_2-trapped trigonal Li_3^+ and Na_3^+ systems were calculated. The frontier molecular orbital pictures were obtained through the GAUSSVIEW 03 package [35].

Results and discussion

Total energy (E, a.u.) and important global reactivity descriptors such as electronegativity (χ), hardness (η) and electrophilicity (ω) for the different H_2-trapped Mg_n and Ca_n cages (n=8–10) are presented in Table 1. A similar display of the above global reactivity descriptors for the different Li_3^+ and Na_3^+-bound poly-hydrogen clusters can be seen in Tables 2 and 3, respectively. The energies of these Li_3^+ and Na_3^+-bound poly-hydrogen clusters optimized at different levels of theory are shown in Tables 4 and 5, respectively. Tables 6, 7 and 8 present a detailed description of the aromaticity measures of the H_2-bound metallic cages and rings computed in terms of $NICS_{zz}$ values. A thorough analysis of the corresponding reaction energies (ΔE) upon increasing H_2-storage by the trigonal, aromatic Li_3^+ and Na_3^+ systems is given in Tables 9 and 10, respectively. An in-depth population analysis study under the Mulliken scheme (MPA) consisting of the atomic charges (Q_k) and FFs (f_k^+,f_k^-) for all the atomic sites of the H_2-bound Mg_n and Ca_n cages (n=8–10), Li_3^+ and Na_3^+ trapped clusters are shown in Tables S1–S3, respectively. Figure 1 depicts the optimized geometries of the different H_2-trapped Mg_n and Ca_n cages (n=8–10). The stable molecular conformations of the different Li_3^+ and Na_3^+-bound poly-hydrogen clusters are portrayed in Figs. 2 and 3, respectively. A variation of the η and ω values for the Li_3^+ and Na_3^+ systems as a function of increasing H_2-

Table 8 $NICS_{ZZ}$ (0, ppm) values of the trigonal Na_3 ring in the different H_2-trapped Na_3^+ clusters

Molecules	NICSzz (0)
Na_3^+	−12.77
H_2-Na_3^+	−8.52
H_4-Na_3^+	−8.49
H_6-Na_3^+	−13.12
H_8-Na_3^+	−11.97
H_{10}-Na_3^+	−13.14

Table 10 Reaction energy (ΔE, kcal mol^{-1}) for the gradual formation of different H_2-trapped Na_3^+ clusters

Reactions	ΔE
$Na_3^+ + H_2 = H_2Na_3^+$	−0.697
H_2-$Na_3^+ + H_2 = H_4Na_3^+$	−0.639
H_4-$Na_3^+ + H_2 = H_6Na_3^+$	−0.569
H_6-$Na_3^+ + H_2 = H_8Na_3^+$	−0.200
H_8-$Na_3^+ + H_2 = H_{10}Na_3^+$	−0.165

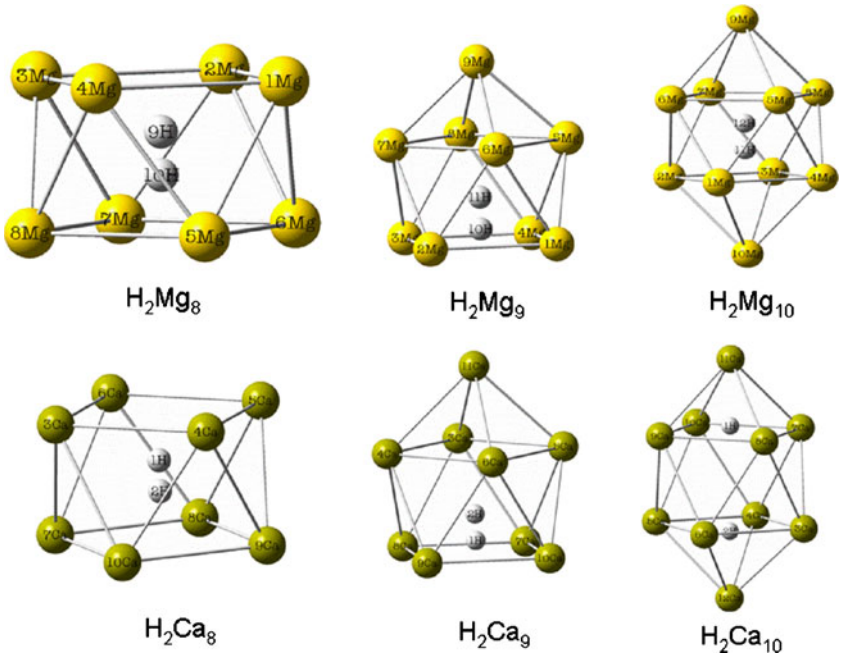

Fig. 1 Optimized geometries (B3LYP/6–311+G(d)) of H_2M_n (where M=Mg, Ca; n=8, 9, 10) clusters

trapping is plotted in Figs. 4 and 5, respectively. The important frontier molecular orbitals (FMOs) of the H_2-trapped Mg_n and Ca_n cages (n=8–10) and the Li_3^+ and Na_3^+-bound poly-hydrogen clusters are shown in supporting information as Figs. S1–S3, respectively.

Scrutiny of Table 1 reveals that the energies of the H_2-bound Mg_n and Ca_n cages (n=8–10) increase, as expected. It may, however, be noted that the Mg_n/Ca_n cages cannot be stabilized in the free, unbound form until molecular hydrogen are trapped within them. This aspect can be seen clearly in Fig. 1. Figure 1 further illustrates that in the Ca_{10} cage, unlike other cages, the H–H distance increases and hydrogen is bound mainly in its atomic form. Tables 2 and 3 reveal that the electrophilicity (ω) of the different conformations of Li_3^+ and Na_3^+-bound poly-hydrogen clusters decreases gradually upon increasing the number of trapped H_2 molecules. This trend possibly warrants the increasing stability of the H_2-trapped Li_3^+ and Na_3^+ systems upon increase in the cluster size, thereby providing some theoretical justification towards the use of such trigonal alkali-metal systems as storage materials for hydrogen. The varied geometrical conformations of the poly-hydrogen bound Li_3^+ and Na_3^+ complexes illustrated in Figs. 2 and 3, respectively, also show that H_2 molecules captured in the

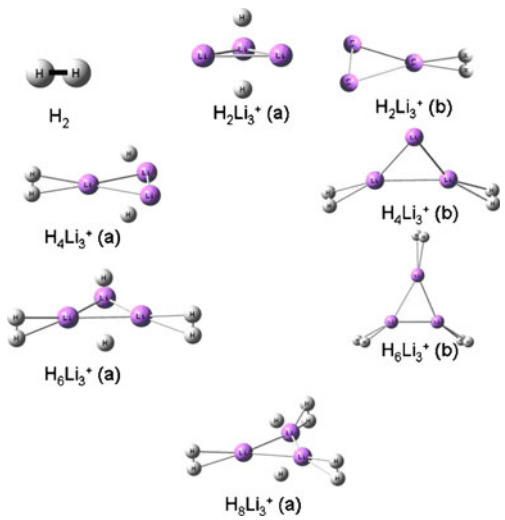

Fig. 2 Geometries of the different hydrogen trapped Li_3^+ (types a and b) clusters optimized at B3LYP/6–311+G(d) level of theory

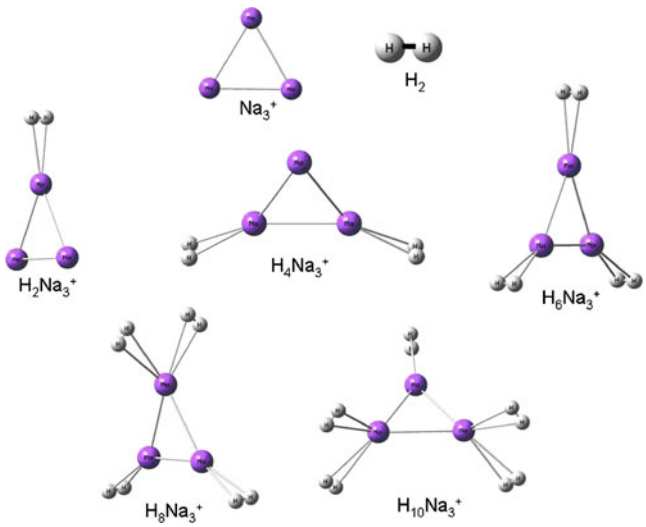

Fig. 3 Geometries of the different hydrogen trapped Na_3^+ clusters optimized at B3LYP/6–311+G(d) level of theory

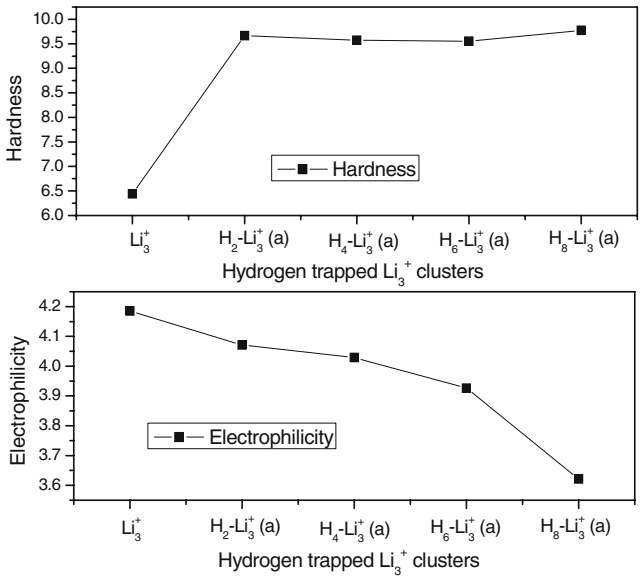

Fig. 4 Variation of hardness (η) and electrophilicity (ω) for gradual trapping of H_2 to form H_n-Li_3^+ (type a) clusters

trigonal ring mostly dissociate and are eventually trapped in atomic form, while those bound at the apices retain their diatomic, rather molecular nature. Tables 4 and 5 further reveal that the structures of all the conformers of H_2-bound Li_3^+ and Na_3^+ clusters optimized at different higher levels of theory are stabilized upon gradual trapping. Tables 6, 7 and 8 illuminate the stabilization of the H_2-bound metal clusters in terms of NICS [26], an aromaticity criterion often executed successfully to determine the stability of all-metal ring systems. Table 6 shows that both the NICS(0) and NICS(1) values for the upper and lower rings of the H_2-trapped Mg_n and Ca_n cages (n=8–10) are negative, which proves the existence of a diatropic ring current in the M_4 (M = Mg, Ca) rings of the clusters. Tables 7 and 8 reveal a similar aromatic stabilization in the free as well as poly-hydrogen bound clusters of the different conformations of Li_3^+ and Na_3^+ species. From Tables 9 and 10, it is evident that the reaction energy, (ΔE, kcal mol^{-1}) for the gradual uptake of H_2 by the aromatic Li_3^+ and Na_3^+ clusters is negative. The negative ΔE values perhaps provide some support of gradual H_2-binding by the Li_3^+ and Na_3^+ clusters from a thermodynamic viewpoint. However, the ΔE values for higher order H_2-trapping with increasing numbers of H_2 molecules is several times lower for the Na_3^+ system compared to Li_3^+. This may be rationalized from the smaller size and hence a higher charge density of the Li^+ species compared to Na^+, which provokes the former to attract H_2 molecules a bit more strongly than the latter.

A detailed scrutiny of the local parameters exhibited in Tables S1–S3 for all the hydrogen-bound metal cages and clusters shows that the atomic charges (Q_k) on the metal centers for the Mg_n and Ca_n cages (n=8–10) are mostly positive, particularly for metal sites present in the upper and lower rings. These centers therefore may become the targets of anions and hard nucleophilic attack upon chemical response. All the metal centers for H_2Mg_8 and some sites for H_2Mg_9, H_2Mg_{10} and H_2Ca_{10} bear negative charges, thereby presuming an electrophilic attack. All the metal centers for the trigonal Li_3^+ and Na_3^+ rings in the H_2-trapped complexes bear positive charges, and therefore are similarly prone to attack by nucleophilic species. The variation in η and ω values for the different poly-hydrogen bound Li_3^+ and Na_3^+ systems depicted as a function of increasing H_2-trapping in Figs. 4 and 5, respectively, pictorially reveals the uniform decrease in the electrophilicity (ω) values upon cluster growth, justifying the trends observed in Tables 2 and 3. The behavior of η roughly mirrors that of ω, confirming the validity of the PMH [27–29] and the PME [32, 33]. Systems like X_2Y_3 (X = Li, Na, K; Y = Be, Mg, Ca) can also trap H_2 (not shown here). The important frontier orbitals of the H_2-bound Mg_n and Ca_n cages (n=8–10) (see Fig. S1) show that, for n=8, the HOMO is σ-antibonding in nature for both the Mg and Ca cages. For the other cages, the highest occupied MO contours are a bit complex but still depict some electron delocalization surrounding the upper and lower rings. On the other hand, the frontier orbitals of the Li_3^+ and Na_3^+-bound poly-hydrogen clusters (see Figs. S2 and S3, respectively) reveal some interesting trends. The HOMO of the free Li_3^+ (Fig. S2) system shows an expected σ-symmetry as the latter also possesses a σ-aromaticity [36]. The H_2-bound Li_3^+ systems also portray a σ-HOMO when the hydrogens retain their molecular nature (type b) and are coplanar with the trigonal, aromatic Li_3^+

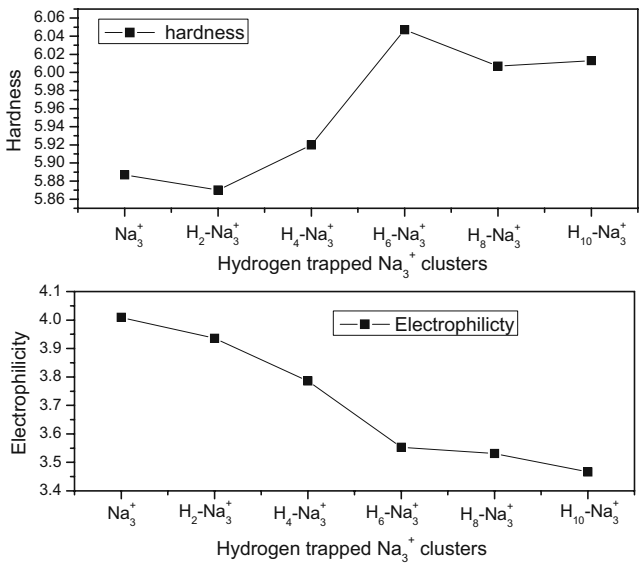

Fig. 5 Variation of hardness (η) and electrophilicity (ω) for gradual trapping of H_2 to form H_n-Na_3^+ clusters

ring. However, for the other isomers, which have a split H_2 molecule trapped mostly in its atomic form (type a), the HOMO exhibits a π-symmetry. In that case the H-atoms of the ripped H_2 molecule lie on a plane perpendicular to that of the Li_3^+ ring. The frontier molecular orbitals of the hydrogen-trapped Na_3^+ complexes (Fig. S3) also represent a similar trend like that of the corresponding type b Li_3^+ analogs. For hydrogen-bound Na_3^+ systems, the H_2 molecule retains its diatomic nature, and thereby remains coplanar with the Na_3^+ ring. The HOMOs thus show a σ-symmetry for the free as well as H_2-trapped Na_3^+ complexes.

Conclusions

The potential use of some alkaline-earth metal cages like Mg_n and Ca_n (n=8–10) as well as a couple of trigonal, aromatic and cationic alkali-metal clusters Li_3^+ and Na_3^+ as trapping/storage materials for H_2 was scrutinized in depth with the aid of conceptual DFT through various global and local reactivity descriptors. The energy (E), hardness (η) and electrophilicity (ω) of the poly-hydrogen bound metal complexes suggest a gradual increment in stability upon cluster growth. The NICS(0,1) for the upper and lower rings of the H_2-bound Mg_n and Ca_n (n=8–10) cages as well as the $NICS_{zz}(0)$ values of the free and hydrogen-trapped Li_3^+ and Na_3^+ rings are negative. Thus, the presence of an "all-metal aromaticity" in the different cages and rings is verified. The stability of the hydrogen-trapped complexes also achieves some thermodynamic support from the negative ΔE values. These all-metal cages and rings can therefore be fruitfully applied as trapping materials for hydrogen—a future fuel reserve.

Acknowledgment The authors thank Indo-EU (HYPOMAP) project for financial assistance

References

1. The Energy White Paper: Our energy future-creating a low carbon economy, Department of Trade and Industry, UK, 2003
2. Song Y, Guo ZX, Yang R (2004) Phys Rev B 69:094205 (1–11)
3. Schlapbach L, Züttel A (2001) Nature 414:353–358
4. Wang Q, Sun Q, Jena P, Kawazoe Y (2009) ACS Nano 3:621–626
5. Shevlina SA, Guo ZX (2006) Appl Phys Lett 89:153104 (1–3)
6. Srinivasu K, Chandrakumar KRS, Ghosh SK (2008) Phys Chem Chem Phys 10:5832–5839, and refs 2–12 therein
7. Peng Q, Chen G, Mizuseki H, Kawazoe Y (2009) J Chem Phys 131:214505 doi:10.1063/1.3268919
8. Wu G, Wang J, Zhang X, Zhu L (2009) J Phys Chem C 113:7052–7057
9. Wagemans RWP, van Lenthe JH, de Jongh PE, van Dillen AJ, de Jong KP (2005) J Am Chem Soc 127:16675–16680
10. McNelles P, Naumkin FY (2009) Phys Chem Chem Phys 11:2858–2861
11. Parr RG, Yang W (1989) Density functional theory of atoms and molecules. Oxford University Press, New York
12. Chattaraj PK (ed) (2009) Chemical reactivity theory: a density functional view. Taylor & Francis/CRC, Florida
13. Geerlings P, De Proft F, Langenaeker W (2003) Chem Rev 103:1793–1874
14. Chattaraj PK, Giri S (2009) Ann Rep Prog Chem Sect C: Phys Chem 105:13–39
15. Sen KD, Jorgenson CK (eds) (1987) Structure and bonding, vol. 66: Electronegativity. Springer, Berlin
16. Chattaraj PK (1992) J Indian Chem Soc 69:173
17. Parr RG, Donnelly RA, Levy M, Palke WE (1978) J Chem Phys 68:3801–3807
18. Sen KD, Mingos DMP (eds) (1993) Structure and bonding, vol. 80: Chemical Hardness. Springer, Berlin
19. Parr RG, Pearson RG (1983) J Am Chem Soc 105:7512–7516
20. Pearson RG (1997) Chemical hardness: applications from molecules to solids. Wiley-VCH, Weinheim
21. Parr RG, Szentpaly Lv, Liu S (1999) J Am Chem Soc 121:1922–1924
22. Chattaraj PK, Sarkar U, Roy DR (2006) Chem Rev 106:2065–2091
23. Chattaraj PK, Roy DR (2007) Chem Rev 107:PR46–PR74
24. Mulliken RS (1955) J Chem Phys 23:1833–1840
25. Parr RG, Yang W (1984) J Am Chem Soc 106:4049–4050
26. Schleyer PvR, Maerker C, Dransfeld A, Jiao H, Hommes NJRvE (1996) J Am Chem Soc 118:6317–6318
27. Pearson RG (1987) J Chem Educ 64:561–567
28. Parr RG, Chattaraj PK (1991) J Am Chem Soc 113:1854–1855
29. Ayers PW, Parr RG (2000) J Am Chem Soc 122:2010–2018
30. Chattaraj PK, Sengupta S (1996) J Phys Chem 100:16126–16130
31. Fuentealba P, Simon-Manso Y, Chattaraj PK (2000) J Phys Chem A 104:3185–3187
32. Chamorro E, Chattaraj PK, Fuentealba P (2003) J Phys Chem A 107:7068–7072
33. Parthasarathi R, Elango M, Subramanian V, Chattaraj PK (2005) Theor Chem Acc 113:257–266
34. Yang W, Mortier WJ (1986) J Am Chem Soc 108:5708
35. Frisch MJ, Trucks GW, Schlegel HB, Scuseria GE, Robb MA, Cheeseman JR, Montgomery JA Jr, Vreven T, Kudin KN, Burant JC, Millam JM, Iyengar SS, Tomasi J, Barone V, Mennucci B, Cossi M, Scalmani G, Rega N, Petersson GA, Nakatsuji H, Hada M, Ehara M, Toyota K, Fukuda R, Hasegawa J, Ishida M, Nakajima T, Honda Y, Kitao O, Nakai H, Klene M, Li X, Knox JE, Hratchian HP, Cross JB, Adamo C, Jaramillo J, Gomperts R, Stratmann RE, Yazyev O, Austin AJ, Cammi R, Pomelli C, Ochterski JW, Ayala PY, Morokuma K, Voth GA, Salvador P, Dannenberg JJ, Zakrzewski VG, Dapprich S, Daniels AD, Strain MC, Farkas O, Malick DK, Rabuck AD, Raghavachari K, Foresman JB, Ortiz JV, Cui Q, Baboul AG, Clifford S, Cioslowski J, Stefanov BB, Liu G, Liashenko A, Piskorz P, Komaromi I, Martin RL, Fox DJ, Keith T, Al-Laham MA, Peng CY, Nanayakkara A, Challacombe M, Gill PMW, Johnson B, Chen W, Wong MW, Gonzalez C, Pople JA (2003) Gaussian 03, Revision B.03; Gaussian Inc.: Pittsburgh, PA
36. Havenith RWA, De Proft F, Fowler PW, Geerlings P (2005) Chem Phys Lett 407:391–396